

Star Tracker Error Characteristics and Their Compensation Techniques

Yeong-Wei (Andy) Wu and Rongsheng (Ken) Li
Boeing Satellite Systems
P. O. Box 92919
Los Angeles, CA 90009-2919

ABSTRACT

A stellar inertial attitude determination (SIAD) system using continuously running gyros and star trackers has been developed within Boeing Satellite Systems (BSS) to support various NASA/government programs. The SIAD performance not only depend on the individual selected gyro and star tracker performance, also are sensitive to the designed attitude determination algorithms such as Kalman filter implemented in the Spacecraft Control Processor (SCP).

Thorough analyses during the course of SIAD development for NASA GOES N program [1] had led us to the following key conclusions: (1) star tracker errors have both temporal noise and spatially dependent noises; (2) these errors are not mutually independent from sample to sample; and (3) the treatment of these errors as independent Gaussian noises in the Kalman filter design can lead to an inferior SIAD performance.

In this paper, we will describe how we characterize the star tracker errors and how we make use of this information to compensate for or deal with these errors in the Kalman filter design so that the SIAD performance can be optimized. Two specific compensation techniques will be described in details in the paper: Kalman filter design optimization [5] and compensation technique for star tracker CTE (Charge Transfer Efficient) induced error [6].

INTRODUCTION

Star trackers have recently been used in many Government and Commercial programs including NASA's GOES N [1], Boeing's Spaceway [2], APL's Midcourse Space Experiment (MSX) [3], Near Earth Asteroid Rendezvous (NEAR), and Thermosphere, Ionosphere, Mesosphere Energetic and Dynamics (TOMED), NASA/Lockheed Martin's Microwave Anisotropy Probe (MAP) [4], and many other Government classified programs. These Charged Coupled Device (CCD) based star trackers are integrated with a 3-axis continuously running gyros system to provide a attitude determination system supporting various high precision satellite pointing missions.

The CCD-based star tracker is an electro-optical device that provides measurements of the position and intensity of stars within its field-of-view (FOV) for the purpose of satellite attitude determination. As shown in Figure 1, the sensor basically consists of: a sunshade, optics, a CCD array, an analog signal processing, a digital signal processing, a power supply, and necessary interfaces. The sunshade, mounted to the front surface of the tracker is used to block out or attenuate stray-light from the sun, earth and moon. The optics focuses incoming starlight onto the CCD array, which is normally cooled to near zero degree C by a thermal-electric cooler (TEC). The CCD converts the received photons to electrical signals. Signals from CCD are then amplified and filtered by an analog signal processor, and digitized for further processing. A digital signal processor performs additional data processing including star image centroiding and validation. The time-tagged star position and star magnitude are sent to the Spacecraft Control Processor (SCP) via “Dual Standby Redundant” 1553B I/O bus. In most applications the star tracker operates as a remote terminal that receives commands from and supplies data to the SCP, which serves as the bus controller.

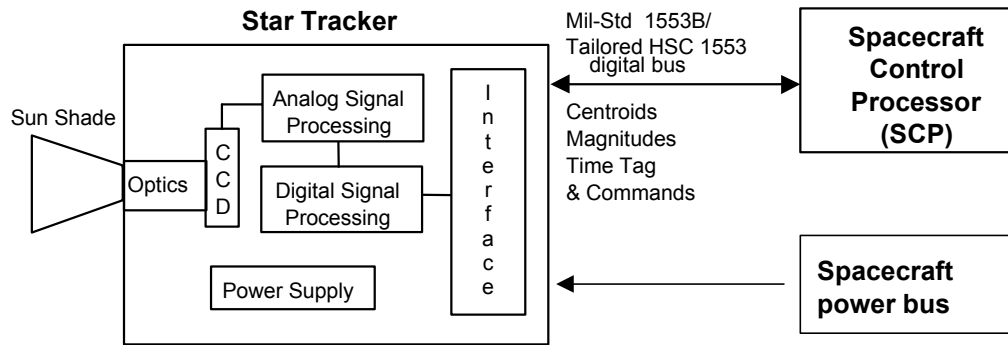


Figure 1. Star Tracker Assembly Interfaces with the Spacecraft

In a typical stellar inertial attitude determination (SIAD) system [1], as shown in Figure 2, the spacecraft inertial attitude is determined continuously in the SCP by numerically integrating the measured spacecraft inertial rates provided by three orthogonal gyros. Periodically the star data (time-tagged star positions and star magnitudes) are then used in the Kalman filter processing to provide corrects compensating both attitude and gyro errors in real time. Thorough analysis had been conducted during the course of SIAD development for the GOES N program. The analysis indicated that the SIAD performance is sensitive to the Kalman filter design and star tracker error characteristics. As also discovered in [3] that: (i) star tracker errors have both temporal noise and spatially dependent noises; (ii) these errors are not necessary mutually independent from sample to sample; and (iii) the treatment of these errors as independent Gaussian noises in the Kalman filter design can lead to an inferior SIAD performance.

In the following we will characterize the star tracker errors and discuss how we compensate for or deal with these errors so that the SIAD performance can be optimized. Two specific compensation techniques will be described in details: Kalman filter design

optimization [5] and compensation technique for star tracker CTE (Charge Transfer Efficient) induced error [6].

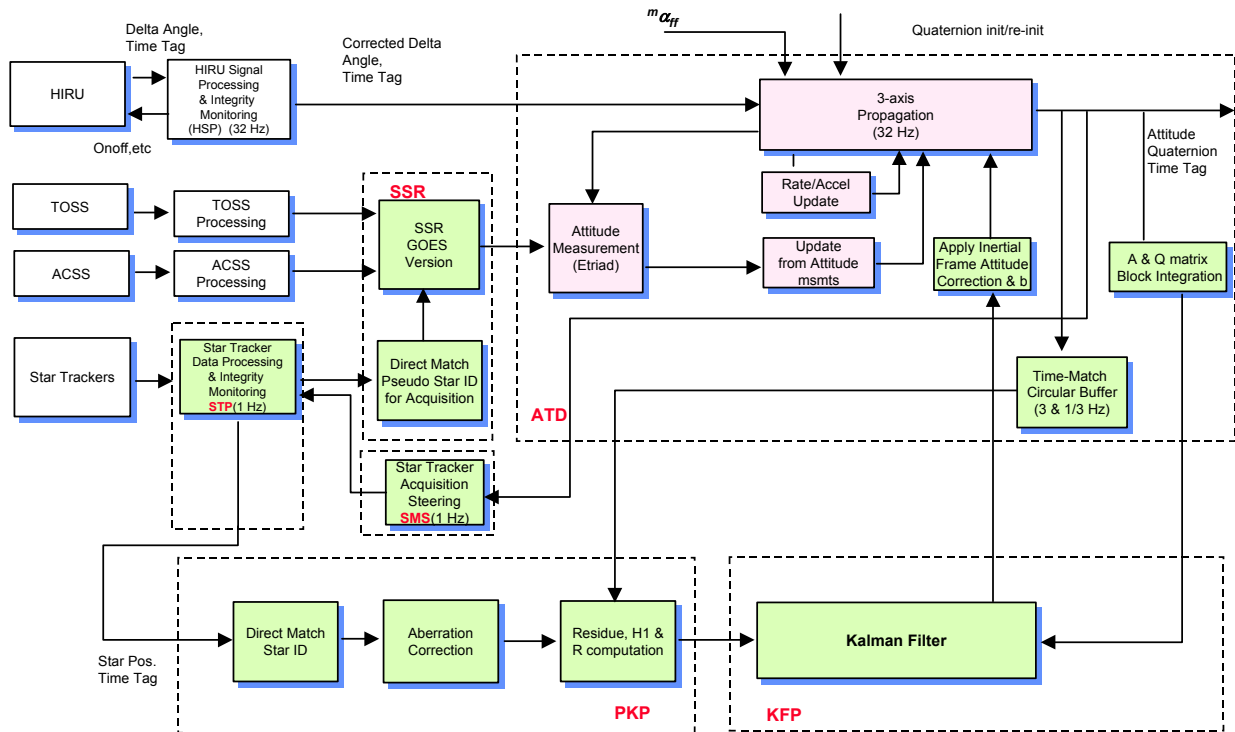


Figure 2. SIAD Subsystem Software Architecture

STAR TRACKER ERROR CHARACTERISTICS

The CCD-base star tracker contains two types of errors: temporal errors and spatially dependent errors. Temporal errors are the frame-to-frame noise when a star is located at a fixed position. Temporal error is also referred to as noise equivalent angle (NEA). Spatially dependent errors are those errors, which depend on the star positions within the tracker FOV.

There are two major sources of temporal errors: shot noise and readout noise. The shot noise is due to the Poisson noise existed in the measured background electrons. The readout noise is the noise in the analog electronics. These noises are independent of star positions.

Spatially dependent errors can be further broken down into low spatial frequency (LSF) errors and high spatial frequency (HSF) errors. LSF errors are systematic errors that have spatial correlation periods on the order of degrees. On the other hand, HSF errors have a spatial correlation period of a few detector widths (in the order of few arc-minutes or less).

The major contributors to the LSF errors are: calibration residuals, color shift induced error, and charged transfer efficiency (CTE) degradation induced error.

Calibration residuals are the difference between the true star positions and the star tracker reported positions after applying corrections established during initial ground calibration. These calibration residuals, ΔH_{LSF} and ΔV_{LSF} expressed in horizontal (h) and vertical (v) positions, can be accurately modeled as a 3rd polynomial function:

$$\Delta H_{LSF} = \alpha(M_i) \sum_{m=0}^3 \sum_{n=0}^{3-m} a_{mn} h^m v^n$$

$$\Delta V_{LSF} = \beta(M_i) \sum_{m=0}^3 \sum_{n=0}^{3-m} b_{mn} h^m v^n$$

where a_{mn} and b_{mn} are constant coefficients chosen to fit the following error surface obtained during initial ground calibration, and α and β are both functions of star magnitude, M_i .

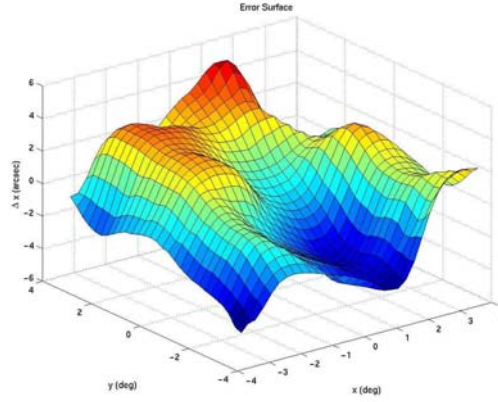


Figure 3. LSF error Surface Generated During Initial Ground Calibration

The color shift error is introduced when the color spectrum of the observed star is different from that of star used to calibrate the spatial errors. Figure 4 shows the star color shift error (relative to G0V star) versus field angle. As shown in the figure the magnitude of star color shift error increases as the field angle increases. However, the maximum error at the field angle limit depends on the spectral class.

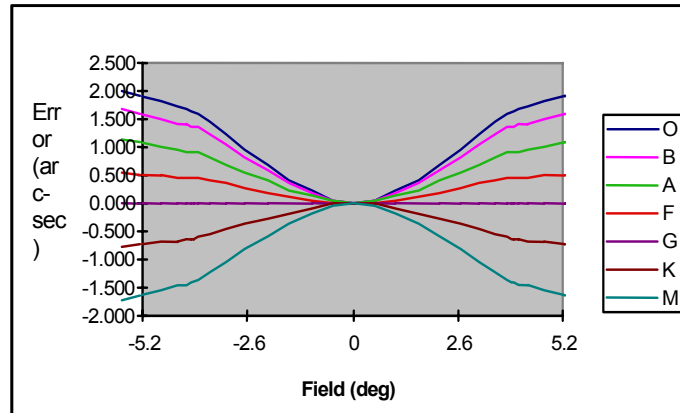


Figure 4. Star Color Shift Error As a Function of Field Angle and Spectral Class

Through charge collection and charge transfer, each CCD provides the conversion of light intensity into measurable voltage signals. As the charge packet moves from one CCD to another CCD, a few electrons are left behind. The ability to transfer all the charges is given by the charge transfer efficiency (CTE). The CTE decreases over the mission life due to displacement damage to the CCD caused by proton radiation. For an image array being transferred down and right, a lower CTE tends to defer the charge packet up and left with respect to the imaging array. As a result, the calculated centroid of the star image shifts up and left. For a given CTE, the resultant centroiding error as a function of number of transfers required to read out the image is shown in Figure 5.

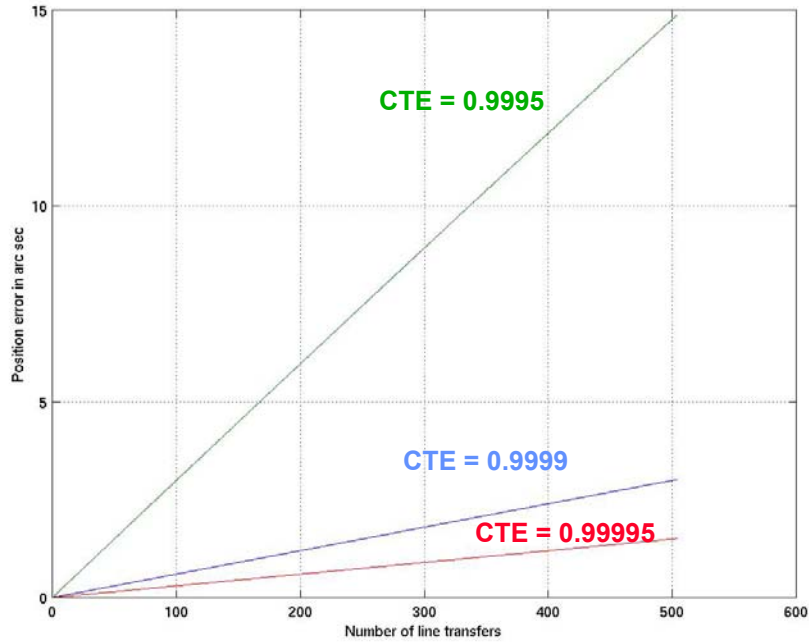


Figure 5. CTE Induced Error Is Proportional To The Number Of Transfers

HSF errors can be broken into random and systematic components. The systematic HSF error is the error in calculating star centroiding position using a finite number of pixels. This so-called “S-curve” error, as shown in Figure 6, has a spatial period of one pixel. Random non-uniformities (dark current and responsivity) in the CCD will cause random HSF errors. These errors will have a correlation period on the order of the size of the image group (about 5 pixels). In general LHF error reduces for brighter stars. Mathematically, the HSF errors, ΔH_{HSF} and ΔV_{HSF} can be expressed as:

$$\Delta H_{HSF} = h_0(M_i) \sin(2\pi f_d + \phi_h)$$

$$\Delta V_{HSF} = v_0(M_i) \sin(2\pi f_d + \phi_v)$$

where h_0 and v_0 are functions of star magnitude M_i , f_d is the spatial frequency, ϕ_h and ϕ_v are the constant phases in pixels.

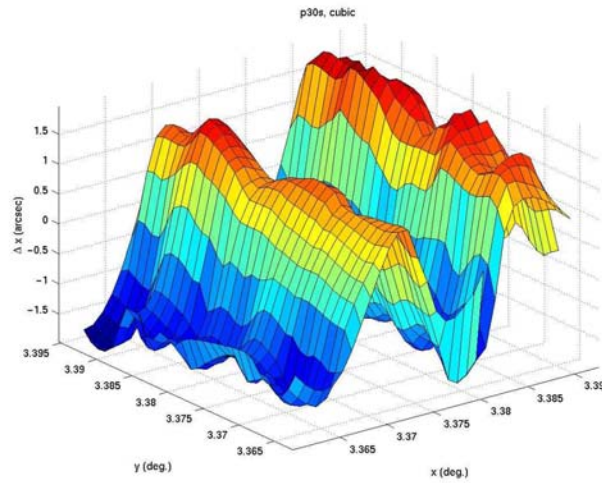


Figure 6. HSF Error Surface as a Function of Pixel Phase

Figure 7 shows the error budget for the Ball CT-602 star tracker used for the GOES N program [1].

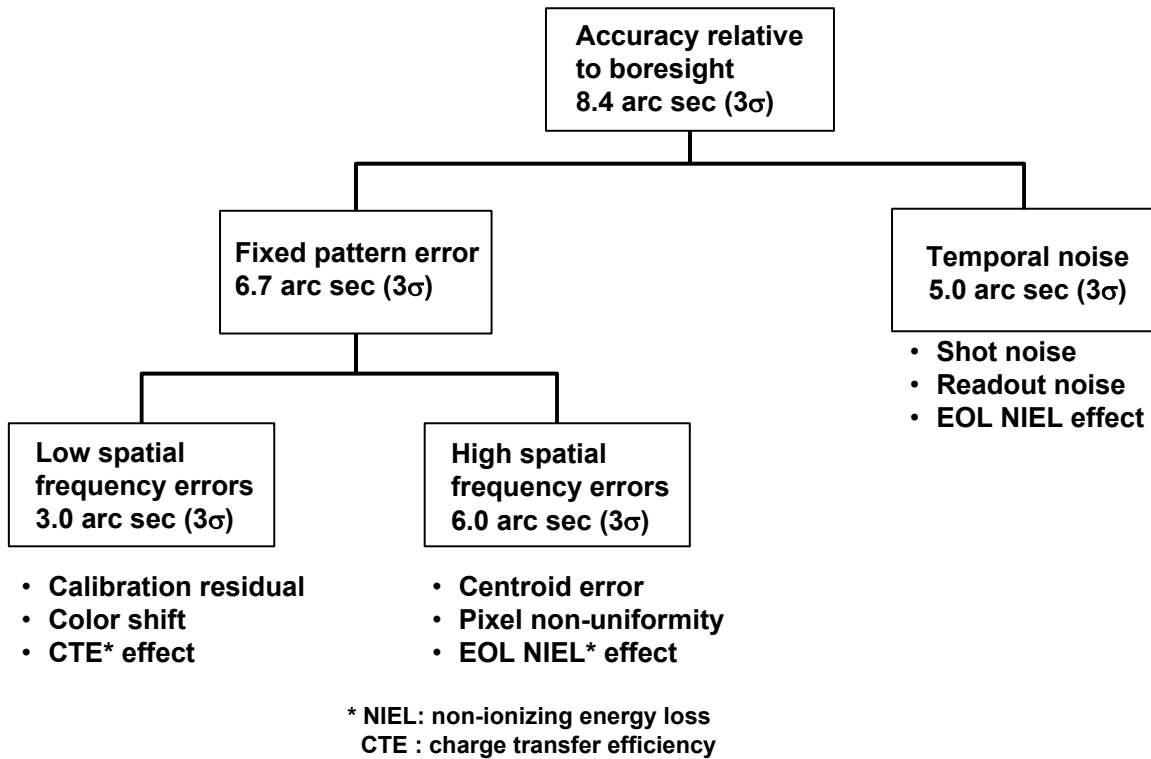


Figure 7 GOES Star-Tracker Error Budget Spec. (per star position accuracy)

R-FACTOR OPTIMIZATION

As discussed in the earlier sections, star position measurement errors cannot be treated as white noises. A colored noise model can be used to more faithfully describe the characteristics of the star-tracker errors but it is very difficult to determine the parameters in a robust and reliable way. In addition, a colored noise model used in a Kalman Filter formulation leads to higher order designs, which is often undesirable. A practice that is typically done at Boeing is to use a Kalman Filter architecture that treats all star-tracker errors as white noises and adjust the “R matrix”, or the measurement covariance matrix, according to the following formulae

$$R = \sigma_{TN}^2 + k_{HSF} \sigma_{HSF}^2 + k_{LSF} \sigma_{LSF}^2$$

where the term σ_{TN}^2 accounts for the contribution of white noises, the term $k_{HSF} \sigma_{HSF}^2$ accounts for the contribution of the high spatial frequency error, the term $k_{LSF} \sigma_{LSF}^2$ accounts for the contribution of the low spatial frequency error. The frequency of the time domain signal is highly dependent on how the stars move across the FOV. The lower the frequency in time domain, the higher the k factor is going to be. Typically $k_{LSF} \gg k_{HSF} > 1$.

In practice, the final result of “R-matrix” is optimized using a simplified covariance model of the overall design and then verified using high fidelity nonlinear simulations. The covariance model uses a high order Markov process to model the time-domain exhibition of the combined high spatial and low spatial frequency errors and solve a Lyapunov equation for the covariance matrix at steady state.

A high order Markov process model is developed by performing spectrum analysis and system identification using the simulated time-domain signal. Figure 8 shows the process and the model. Figure 9 shows a typical plot generated in such a process, and as illustrated, the performance at various “R” values is predicted using the covariance model.

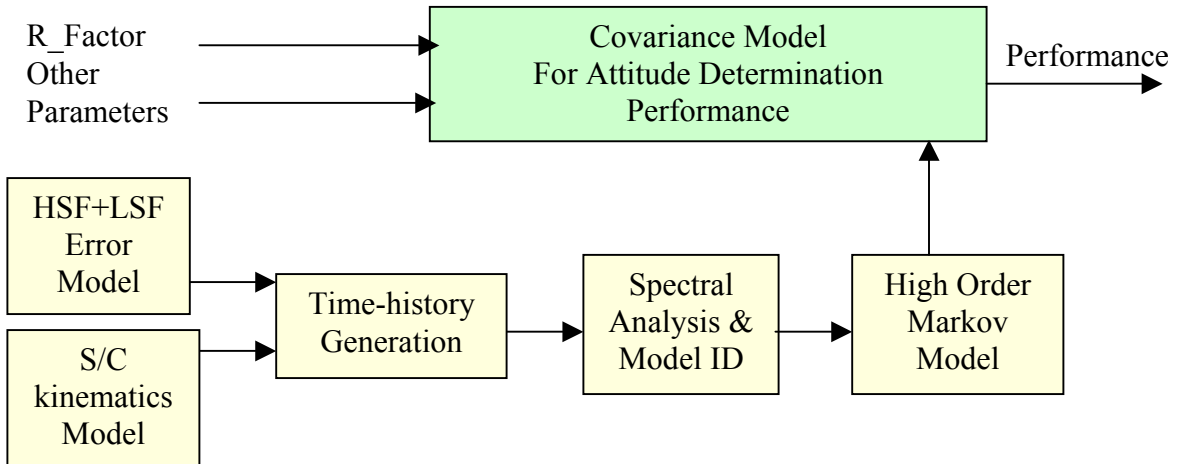


Figure 8. Process and Model Used for R-optimization

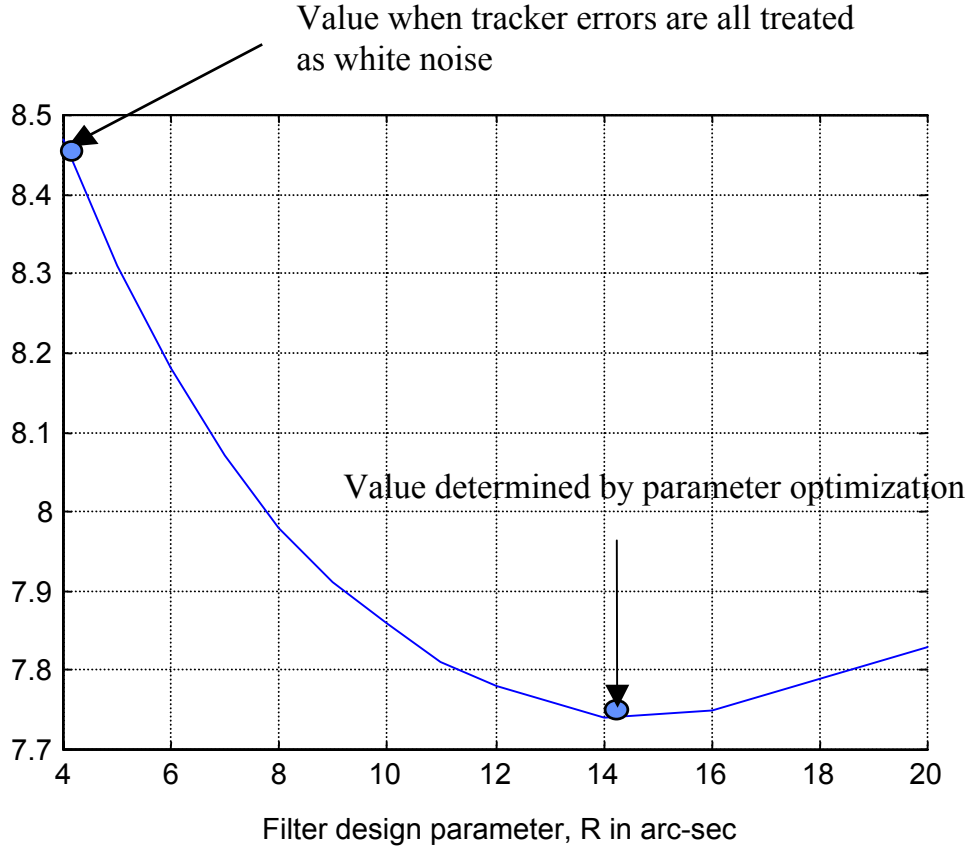


Figure 9. Pitch Attitude Error in Micro Radian as a Function of Value “R”

CTE INDUCED ERROR COMPENSATION

Charge transfer efficiency degrades as radiation dosage accumulates on the CCD array, and is the primary contributor to the low spatial frequency error, which in turn, is the primary error source for an attitude determination system using star-trackers.

Assuming the CCD array is uniformly damaged, the CTE induced error is proportional to the distance the CCD charges have to go through to be shifted for the sampling of the charges. For a multi-port CCD, such as the 4-port CCD as shown in Figure 10, the same CCD charges are transferred out in four different ways. The resulting star centroid position accuracies, which are affected by the charge transfer efficiency, have 4 different values depending on the star locations in the CCD.

Together with star-magnitude information, a math model of the charge transfer efficiency can be parameterized and the parameters can be measured using the 4-port readouts from the CCD array as illustrated in Figure 10. The estimated parameters become reliable after a large amount of star data have been used for the estimation of these parameters. Consequently these parameters can be used to correct the CTE degradation induced low spatial frequency error and lead to significantly improved performance.

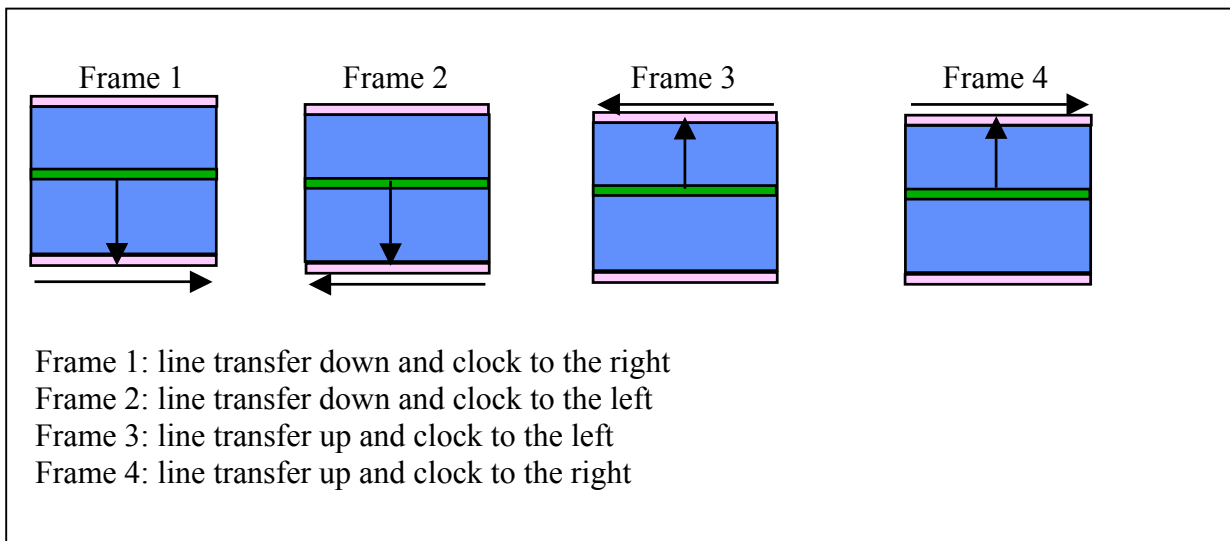


Figure 10. Four –Port CCD Array Readout

Figure 11 describes the signal flow for the CTE error parameter estimation and CTE induced error correction in the overall stellar inertial attitude determination system.

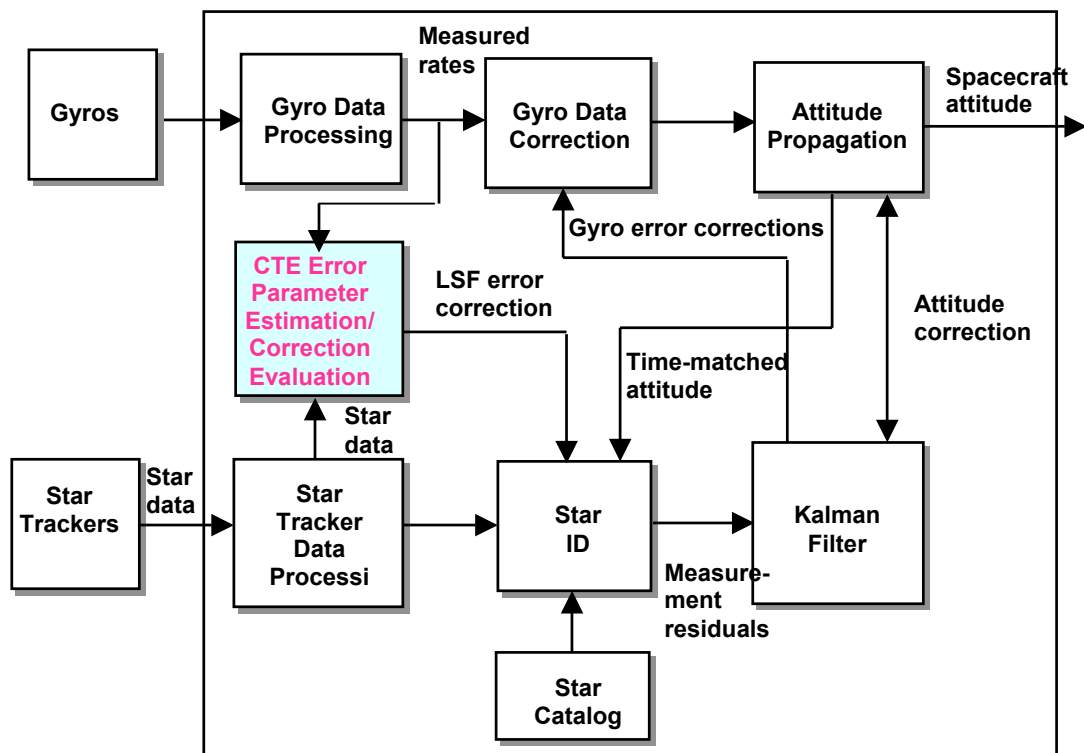


Figure 11. Use of CTE Error Parameter Estimation and Correction in an SIAD System

CONCLUSIONS

Star-tracker error models are critical for both the analysis and the design of star-tracker based attitude determination system. The parameterization of star-tracker errors into temporal noise, high spatial frequency and low-spatial frequency errors helped significantly at Boeing Satellite Systems in developing reliable performance predictions and practical performance optimizations. Recognizing the non-whiteness of the star-tracker errors leads to the “R” optimization technique that was used throughout Boeing satellite programs. Detailed modeling the Charge Transfer Efficiency (CTE) degradation induced errors for star-trackers with multiple read-out ports can lead to a significant performance improvement.

REFERENCES

1. “Precision Attitude Determination for GOES N Satellite”, Andy Wu, Ken Li, and Andrew Robertson, AAS 03-002, 26th Annual AAS Guidance and Control Conference, Breckenridge, Colorado, February 5-9, 2003.
2. “Precision Beacon-Assisted Attitude Control For Spaceway”, Andy Wu, Richard Chiang, and Rongsheng Li, AIAA Guidance, Navigation, and Control Conference, August 11-14, 2003 Austin, Texas.
3. “Attainable Pointing Accuracy with Star Trackers”, D. R. Haley, T. E. Strikwerda, H. L. Fisher, and G. A. Heyler, AAS 98-072.
4. “Performance of the AST-201 Star Tracker for the Microwave Anisotropy Probe”, Roelof van Bezooijen, Kevin Anderson, and David Ward, AIAA Guidance, Navigation, and Control Conference, August 5-8, 2002 Monterey, California.
5. “Enhanced Stellar Attitude Determination System”, US patent #6,047,226, April 4, 2000.
6. “Spacecraft Methods and Systems for Autonomous Correction of Star Tracker Charge Transfer Efficiency Error”, US patent #6,460,809 B1, Oct. 8, 2002.